Available online at www.sciencedirect.com
SCIENCE DIRECT
Bioorganic & Medicinal Chemistry
Bioorganic & Medicinal Chemistry 14 (2006) 6012–6021

Synthesis, characterization, and DNA-binding properties of the Ln(III) complexes with 6-hydroxy chromone-3-carbaldehyde-(2′-hydroxy) benzoyl hydrazone

Bao-dui Wang, Zheng-Yin Yang* and Tian-rong Li

College of Chemistry and Chemical Engineering, State Key Laboratory of Applied Organic Chemistry, Lanzhou University, Lanzhou 730000, PR China

Received 21 March 2006; revised 7 May 2006; accepted 9 May 2006
Available online 14 June 2006

Abstract—A new ligand, 6-hydroxy chromone-3-carbaldehyde-(2′-hydroxy) benzoyl hydrazone (L), was prepared by condensation of 6-hydroxy-3-carbaldehyde chromone (CDC) with 2-hydroxy benzoyl hydrazine. Its four rare earth complexes have been synthesized and characterized on the basis of elemental analyses, molar conductivities, mass spectra, ^{1}H NMR, thermogravimetry/differential thermal analysis (TG–DTA), UV–vis spectra, fluorescence spectra, and IR spectra. The general formula of the complexes is $[LnL_2{\cdot}(NO_3)_2]{\cdot}NO_3$ [Ln = La(**1**), Sm(**2**), Dy(**3**), Eu(**4**)]. Spectrometric titration, ethidium bromide displacement experiments, and viscosity measurements indicate that Eu(III) complex and ligand, especially the Eu(III) complex, strongly bind with calf-thymus DNA, presumably via an intercalation mechanism. The intrinsic binding constants of Eu(III) complex and ligand with DNA were 3.55×10^6 and 1.33×10^6 M^{-1} through fluorescence titration data, respectively. In addition, the suppression ratio for $O_2^{-\cdot}$ and $OH^{\cdot}$ of the ligand and its complexes was studied by spectrophotometric methods. The experimental results show that La (**1**), Sm (**2**), and Eu (**4**) complexes are better effective inhibitor for $OH^{\cdot}$ than that of mannitol. It indicates that the complexes have the activity to suppress $O_2^{-\cdot}$ and $OH^{\cdot}$ and exhibit more effective antioxidants than ligand alone.

1. Introduction

The malignant tumor has long been one of the serious diseases threatening human health. To discover and develop novel therapeutic agents for the treatment of malignancy has a vital importance. One of the successful and effective approaches in the search for new antitumor agents from natural products is to synthesize novel compounds by simple chemical modification on the basis of natural leading compounds.

Chromones are a group of naturally occurring compounds that are ubiquitous in nature especially in plants.[1] They are oxygen-containing heterocyclic compounds with a benzo-annelated γ-pyrone ring, with the parent compound being chromone (4*H*-chromen-4-one, 4*H*-1-benzopyran-4-one).[2] Molecules containing the chromone structure (for example, chromones and flavonoids) have a wide range of biological activities including tyrosine and protein kinase C inhibitors, antifungal, antiallergenic, antiviral, antitublin, antihypertensive, and anticancer agents, as well being active at benzoazepine receptors, lipoxygenase, cyclooxygenase and modulating P-glycoprotein-mediated (MDR).[2–5] Due to their abundance in plants and their low mammalian toxicity, chromone derivatives are present in large amounts in the diet of human.

The interactions of metal complexes with DNA have been the subject of interest for the development of anticancer drugs and effective chemotherapeutic agents for numerous diseases. Of these studies, the interaction of fluorescent transition metal complexes containing multidentate aromatic ligands, with DNA has gained much attention.[6]

Abbreviations: CT-DNA, calf thymus DNA; L, 6-hydroxy chromone-3-carbaldehyde-(2′-hydroxy) benzoylhydrazone; Tris, Tris(hydroxymethyl)-aminomethane; NMR, nuclear magnetic resonance; NBT, nitroblue tetrazolium; MET, methionine; $VitB_2$, vitamin B_2; EB, ethidium bromide; CDC, 6-hydroxy-3-carboxaldehyde chromone; UV–vis, ultraviolet and visible; TG–DTA, thermogravimetry/differential thermal analysis.

Keywords: 6-Hydroxy chromone-3-carbaldehyde-(2′-hydroxy) benzoyl hydrazone; Rare earth complexes; DNA binding.

* Corresponding author. Fax: +86 931 8912582; e-mail: yangzy@lzu.edu.cn

0968-0896/$ - see front matter © 2006 Elsevier Ltd. All rights reserved.
doi:10.1016/j.bmc.2006.05.015

Fluorescent transition metal centers are particularly attractive moieties for such research for not only do they exhibit well-defined coordination geometries but they also often possess distinctive electrochemical or photophysical properties, thus enhancing the functionality of the binding agent.[7] Complexes have found a plethora of applications ranging from foot-printing agents to probes of electron transfer processes within DNA. Further, the application of these molecules necessitates isolation of structurally analogous complexes with different shapes and electronic properties, investigation of their DNA-binding properties, and then the precise understanding of the structural details of their mode of interaction with the target molecule, namely, double helical DNA.

In order to develop new antitumor drugs, which specifically target DNA, it is necessary to understand the different binding modes a complex is capable of undertaking. Basically, metal complexes interact with the double helical DNA in either a non-covalent or a covalent way. The former way includes three binding modes: intercalation, groove binding, and external static electronic effects. Among these interactions, intercalation is one of the most important DNA-binding modes as it invariably leads to cellular degradation. It was reported that the intercalating ability increases with the planarity of ligands.[8,9] (Additionally, the coordination geometry and ligand donor atom type also play key roles in determining the binding extent of complexes to DNA.)[10,11] The metal ion type and its valence, which are responsible for the geometry of complexes, also affect the intercalating ability of metal complexes to DNA.[12,13]

Our previous work showed that the rare earth complexes of 4′,5,7-trihydroxy-flavanone benzoyl hydrazone have certain antioxidant and cytotoxic activity, and can bind to CT-DNA by intercalation.[14,15] In order to continue researching antioxidative activities and DNA-binding model of the flavone benzoyl hydrazone and its complexes, in this paper, we synthesized a new ligand, 6-hydroxy chromone-3-carbaldehyde-(2′-hydroxy) benzoyl hydrazone (Fig. 1), and its rare earth complexes. We described a comparative study of the interactions of Eu(III) complex and ligand with CT-DNA using UV–vis, fluorescence, and viscosity measurements for the first time. The antioxidant activity of the ligand and its rare earth complexes was also investigated. Information obtained from this study will be helpful to the understanding of the mechanism of interactions of chromone hydrazones and their complexes with nucleic acids, and should be useful in the development of potential probes of DNA structure and conformation, and new therapeutic regeants for some diseases.

2. Results

The complexes were prepared by direct reaction of ligand with the appropriate mole ratios of Ln(III) nitrate in ethanol. The yields were good to moderate. The desired Ln(III) complexes were separated from the solution by suction filtration, purified by washing several times with ethanol. The complexes are air-stable for extended periods and soluble in methanol, DMSO, and DMF; slightly soluble in ethanol; insoluble in benzene, water, and diethyl ether. The molar conductivities of the complexes are around 102–104 S cm^2 mol^{-1} in DMF, showing that all complexes are 1:1 electrolytes.[16] The elemental analyses and molar conductivities show that formulas of the complexes conform to [Ln $L_2 \cdot (NO_3)_2] \cdot NO_3$ [Ln = La(**1**), Sm(**2**), Dy(**3**), Eu(**4**)].

2.1. IR spectra

The IR spectra of the complexes are similar. The $\nu_{(hydrazonic)}$ (C=O) and $\nu_{(carbonyl)}$ (C=O) vibrations of the free ligand are at 1646 and 1624 cm^{-1}, respectively; for the complexes these peaks shift to 1634 and 1609 cm^{-1}, $\Delta\nu_{(ligand-complexes)}$ is equal to 12 and 15 cm^{-1}. The band at 600 cm^{-1} is assigned to ν (M–O). These shifts and the new band demonstrate that the oxygen of carbonyl has formed a coordinative bond with the rare earth ions. The different shifts of the wave numbers indicate that the Ln–O (carbonyl) bond is stronger than the Ln–O (hydrazonic) bond. The band at 1596 cm^{-1} for the free ligand is assigned to the ν

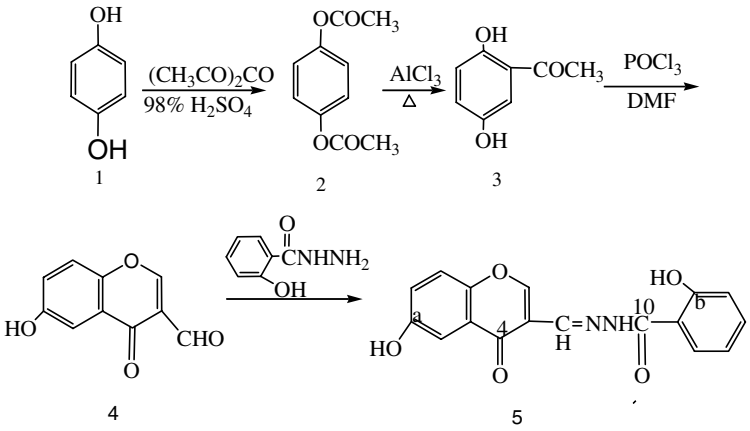

Figure 1. Scheme of the synthesis of the ligand.

(C=N) stretch, which shifts to 1570 cm^{-1} for its complexes. Weak bands at 427 cm^{-1} are assigned to ν (M–N). These shifts and the new band further confirm that the nitrogen of the imino-group bonds to the rare earth ions. The absorption bands of the coordinated nitrates were observed at about 1479 (ν_{as}) and 840 (ν_s) cm^{-1}. The ν_3 (E′) free nitrates appear at 1383 cm^{-1} in the spectra of the complexes. In addition, the separation of the two highest frequency bands $|\nu_4-\nu_1|$ is approximately 155 cm^{-1}, and accordingly the coordinated NO_3^- ion in the complex is a bidentate ligand.[17]

2.2. UV spectra

The study of the electronic spectra in the ultraviolet and visible ranges for the Ln(III) complexes and ligand was carried out in a buffer solution. The electronic spectra of ligand had a strong band at λ_{max} = 244 nm, a medium band at λ_{max} = 290 nm, and a weak band at λ_{max} = 321 nm. The complexes also yield three bands, and the two bands at 290 and 321 nm are shifted to 294 and 324 nm or so. These indicate that complexes are formed.

2.3. Thermal analyses

The complexes begin to decompose at 251 °C or so and there are three exothermic peaks appearing around 237–392 °C. The corresponding TG curves show a series of weight loss. Under 200 °C, there are no endothermic peak and no weight loss on corresponding TG curves. It indicates that there are no crystal or coordinate solvent molecules. While being heated to 800 °C, the complexes become their corresponding oxides. The residues are in accordance with calculation.

2.4. Fluorescence studies

The fluorescence characteristics of the Eu(III) complex in solid form are listed in Table 1. The solid complexes have characteristic line emission of f–f transitions of metal ions when they are excited with UV light. The solid Eu(III) complex shows strong fluorescence emission. Based on the theory of antenna effect,[18,19] the intensity of the luminescence of Ln^{3+} complexes is related to the efficiency of the intramolecular energy transfer between the triple level of the ligand and the emitting level of the ions, which depends on the energy gap between the two levels. In the solid state, probably the energy gap between the ligand's triplet levels and the emitting levels of the Eu(III) favors the energy transfer process for europium. This makes the Eu(III) complex show the most intense red fluorescence. However, the Sm, Dy, and Tb(III) complexes do not exhibit fluorescence, which indicates that energy transfer process between the ligands' triplet levels and the emitting levels of the Sm, Dy, and Tb(III) is not favored.

Table 1. Fluorescence data of the Eu(III) complex at room temperature

Complexes	State	Slit (nm)	λ_{ex} (nm)	λ_{em} (nm)	RFI[a]	Assignment
4	Solid			579.2	19.65	$^5D_0 \rightarrow {}^7F_0$
		2.5	344	592.6	202.00	$^5D_0 \rightarrow {}^7F_1$
				616.6	419.40	$^5D_0 \rightarrow {}^7F_2$
	DMSO	5.0	379	591.6	98.11	$^5D_0 \rightarrow {}^7F_1$
				613.2	51.08	$^5D_0 \rightarrow {}^7F_2$
	DMF			591.1	53.11	$^5D_0 \rightarrow {}^7F_1$
				615.4	38.38	$^5D_0 \rightarrow {}^7F_2$

[a] RFI is relative fluorescence intensity.

The influence of solvent on the fluorescence intensities of the Eu(III) complex was investigated. As given in Table 1, the fluorescence intensities of the Eu(III) complex in organic solvent are weaker than that of powder. This may be due to the quenching process of solvent molecules in the solution. The fluorescence intensity order of the Eu(III) (at the same concentration) in different solvents is DMSO > DMF > CH_3OH (completely quenched). The values ε of three solvents are 46.7 (DMSO), 32.63 (CH_3OH), and 37.6 (DMF). It can be seen that the ε values of these solvents that contain oxygen atom are arranged in the order of 46.7 (DMSO) > 32.63 (CH_3OH). The order of fluorescence intensities in these solvents is in agreement with the ε values of them. This indicates that the polarity of the solvents affects both the absorption and fluorescent intensities of the complex.

2.5. Electronic absorption titration

Before reacting Eu(III) complex with CT-DNA, its solution behavior in buffer solution at room temperature was monitored by UV–vis spectroscopy for 24 h. Liberation of the ligand was not observed under these conditions. These suggest that the complexes are stable under the conditions studied.

The absorption spectra of ligand and Eu(III) complex in the absence and presence of CT-DNA are given in Figure 2a and b, respectively. There exist in Figure 2a three well-resolved bands at 244, 290, and 321 nm for ligand, and in Figure 2b three well-resolved bands at 245, 294, and 324 nm for Eu(III) complex. With increasing DNA concentrations, the hypochromisms increased up to 66.37% at 244 nm and 6.17% at 321 nm for Eu(III) complex; 50.19% at 244 nm and 19.53% at 321 nm for ligand. The hypochromisms observed for the bands of Eu(III) complex and ligand are accompanied by a small red shift by less than 4 nm.

2.6. Fluorescence spectra

The Eu(III) complex and ligand can emit weak luminescence in Tris buffer with a maximum wavelength of about 449 nm for Eu(III) complex and 410 nm for ligand. Emission titrations for the Eu(III) complex and ligand with DNA are illustrated in Figure 3. Compared to the Eu(III) complex and ligand alone, the emission intensity increases with increasing concentrations of CT-DNA.

The emission spectra of EB and DNA-bound EB in the absence and the presence of Eu(III) complex and free ligand are given in Figure 4a and b, respectively.

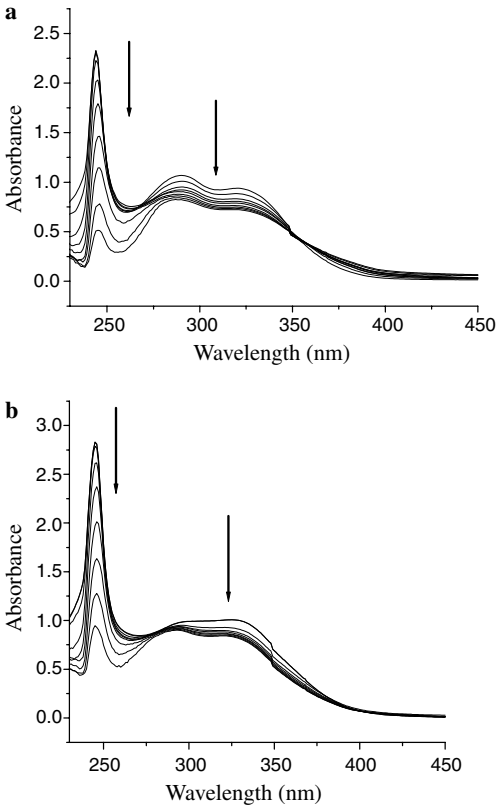

Figure 2. (a) Electronic spectra of ligand (10 μM) in the presence of increasing amounts of CT-DNA. [DNA] = 0–70 μM. Arrow shows the absorbance changes upon increasing DNA concentration. (b) Electronic spectra of Eu(III) complex (5 μM) in the presence of increasing amounts of CT-DNA. [DNA] = 0–80 μM. Arrow shows the absorbance changes upon increasing DNA concentration.

The addition of the Eu(III) complex and free ligand to the DNA-bound EB solutions caused obvious reduction in emission intensities. The quenching plots illustrate that the quenching of EB bound to DNA by the ligand and the complex is in good agreement with the linear Stern–Volmer equation.

2.7. Viscosity studies

The effects of both compounds on the viscosity of DNA are shown in Figure 5. The viscosities of the DNA increase steadily with increasing concentrations of ligand and Eu(III) complex, and the extent of the increase observed for the ligand is smaller than that for the Eu(III) complex.

2.8. Suppression ratio (%) for $O_2^{-\cdot}$ and $OH^{\cdot}$

The data of the suppression ratio for $O_2^{-\cdot}$ are listed in Table 2. We find that the inhibitory effect of the compounds tested on $O_2^{-\cdot}$ is concentration dependent, and the suppression ratio increases with increasing sample concentrations in the range tested (Fig. 6). The average suppression ratio of the ligand (IC_{50} = 65.06 ± 0.62 μM) for $O_2^{-\cdot}$ is the least in all compounds. The Dy(III) complex (**3**) (IC_{50} = 28.08 ± 0.35 μM) is the most effective in the four complexes, whereas the Eu(III) complex (**4**) (IC_{50} = 58.89 ± 0.99 μM) has the poorest inhibitory effect.

The comparison of the inhibitory effect on $OH^{\cdot}$ is shown in Table 3. We can find that all compounds scavenge $OH^{\cdot}$ also in a concentration-dependent manner (Fig. 7). The order of the suppression ratio of tested compounds for $OH^{\cdot}$ is **4** > **2** > **1** > mannitol > **3** > **L**.

3. Discussion

3.1. Structure of the Ln(III) complexes

Since the crystal structure of the Ln(III) complexes has not been obtained yet, we characterized the complexes and determined its possible structure by elemental analyses, molar conductivities, fluorescence data, IR data, TG–DTA, and UV–vis measurements. The likely structure of the complexes is shown in Figure 8.

3.2. DNA-binding constant and mode

The design of small complexes that bind and react at specific sequences of DNA becomes important. A more complete understanding of how to target DNA sites with specificity will lead not only to novel chemotherapeutics but also to a greatly expanded ability for chemists to probe DNA and to develop highly sensitive diagnostic agents.[6]

Transition-metal complexes are being used at the forefront of many of these efforts. Stable, inert, and water-soluble complexes containing spectroscopically active metal centers are extremely valuable as probes of biological systems. As both spectroscopic tags and functional models for the active centers of proteins, metal complexes have helped elucidate the mechanisms by which metalloproteins function.[6]

Large hypochromism of an aromatic dye in presence of double helical DNA is usually characteristic of intercalation into DNA base pairs for the dye, due to the strong stacking interaction between the aromatic chromophore and the base pairs.[20,21] So, the above phenomena imply that the compound interacts with calf thymus DNA quite probably by intercalating the ligand into the base pairs. The binding constant K_b, has been estimated to be $1.76 \times 10^4\ M^{-1}$ (ligand) and $2.49 \times 10^4\ M^{-1}$ (Eu(III) complex), respectively.

In order to test if the Eu(III) complex could bind to DNA by intercalation, ethidium bromide (EB) was employed, as EB interacts with DNA as a typical indicator of intercalation.[22] Figure 9 shows that the maximal absorption of EB at 479 nm decreased and shifted to 515 nm in the presence of DNA, which is characteristic of intercalation. Figure 9c is the absorption of a mixture solution of EB, Eu(III) complex, and DNA. It was found that the absorption at 515 nm increased compared with Figure 9b. This could result from two reasons: (1) EB bound to the Eu(III) complex strongly, resulting in a decreased amount of EB intercalated into

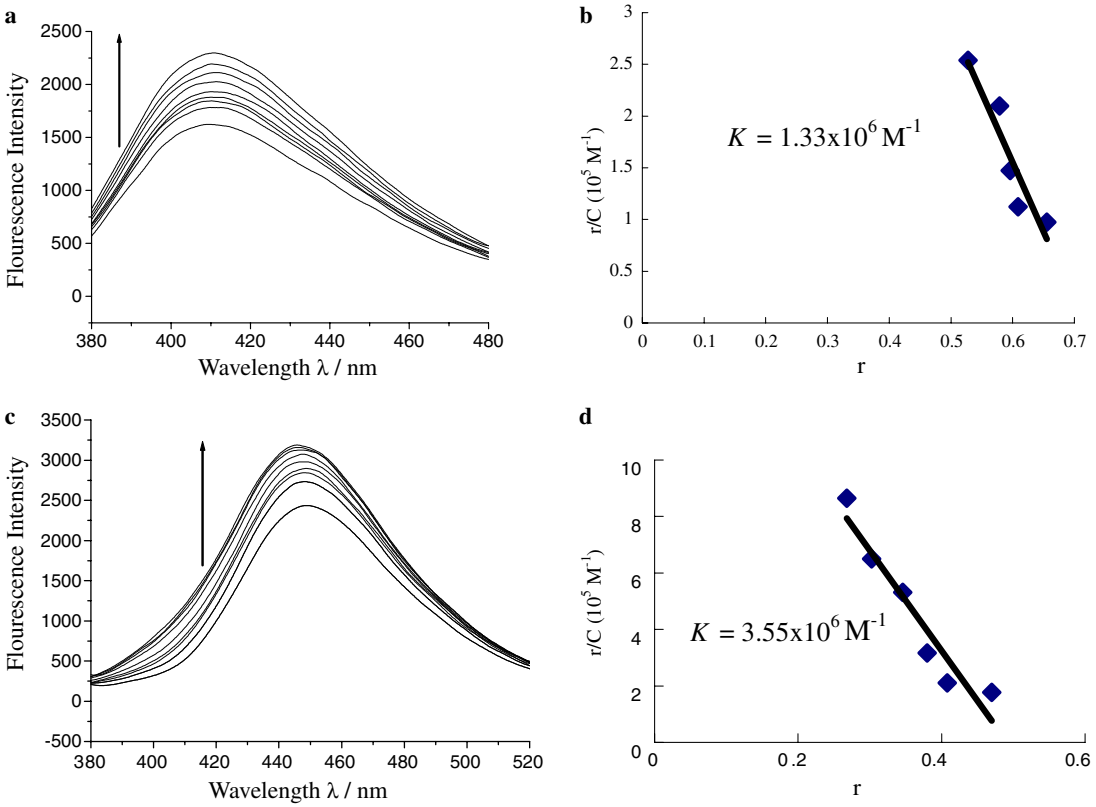

Figure 3. (a) The emission enhancement spectra of ligand (10 μM) in the presence of 0, 2.5, 5, 7.5, 10, 12.5, 15, and 17.5 μM CT-DNA. Arrow shows the emission intensity changes upon increasing DNA concentration. (b) Scatchard plot of the fluorescence titration data of ligand, $K = 1.33. \times 10^6\ M^{-1}$. (c) The emission enhancement spectra of Eu(III) complex (5 μM) in the presence of 0, 2.5, 5, 7.5, 10, 12.5, 15, 17.5 and 20 μM CT-DNA. Arrow shows the emission intensities upon increasing DNA concentration. (d) Scatchard plot of the fluorescence titration data of Eu(III) complex, $K = 3.55 \times 10^6\ M^{-1}$.

DNA; (2) there exists competitive intercalation between the Eu(III) complex and EB with DNA, thus releasing some free EB from DNA–EB system. However, the former reason could be precluded since there were no new absorption peaks.

The results of the emission titrations suggest that both the compounds are protected from solvent water molecules by the hydrophobic environment inside the DNA helix. This implies that both the compounds can insert between DNA base pairs deeply. Since the hydrophobic environment inside the DNA helix reduces the accessibility of solvent water molecules to the compound and the compound mobility is restricted at the binding site, a decrease of the vibrational modes of relaxation results. The binding of the Eu(III) complex and ligand to DNA leads to a marked increase in the emission intensity which also agrees with those observed for other intercalators.[23] According to the Scatchard equation, a plot of r/C_f versus r gave the binding constants 3.55×10^6 and $1.33 \times 10^6\ M^{-1}$ from the fluorescence data for the Eu(III) complex and the free ligand, respectively. These results show that the complex binds more strongly than the free ligand. The higher binding affinity of complex is probably attributed to the extension of the π system of the intercalated ligand due to the coordination of Eu, which also leads to a planar area greater than that of the free ligand, which leads to the coordinated ligand penetrating more deeply into, and stacking more strongly with the base pairs of the DNA.

Competitive binding to DNA of the complexes with ethidium bromide (EB) could provide rich information regarding DNA-binding nature and relative DNA-binding affinity. EB emits intense fluorescence in the presence of DNA, due to strong intercalation between the adjacent DNA base pairs of DNA ($K_b = 1.4 \times 10^6\ M^{-1}$).[24] It was previously reported that the enhanced fluorescence could be quenched, at least partially, by addition of a second intercalative molecule.[25,26] The quenching extents of fluorescence of EB bound to DNA are used to determine the relative DNA-binding affinities of the second molecules. The emission band at 578 nm of the DNA–EB system decreased in intensity with an increase in the concentration of the two compounds, which indicated that the compounds could displace EB from the DNA–EB system. The resulting decrease in fluorescence was caused by EB changing from a hydrophobic environment to an aqueous environment.[27] Such a characteristic change is often observed in intercalative DNA interactions.[28] In the plots of F_0/F versus [Q], K_q is given by the ratio of the slope to the intercept. The K_q values for the Eu(III) complex and ligand are 7.08×10^3 and $4.89 \times 10^3\ M^{-1}$, respectively. The data show that the interaction of the Eu(III) complex with DNA is stronger than that of the free ligand, which is consistent with the

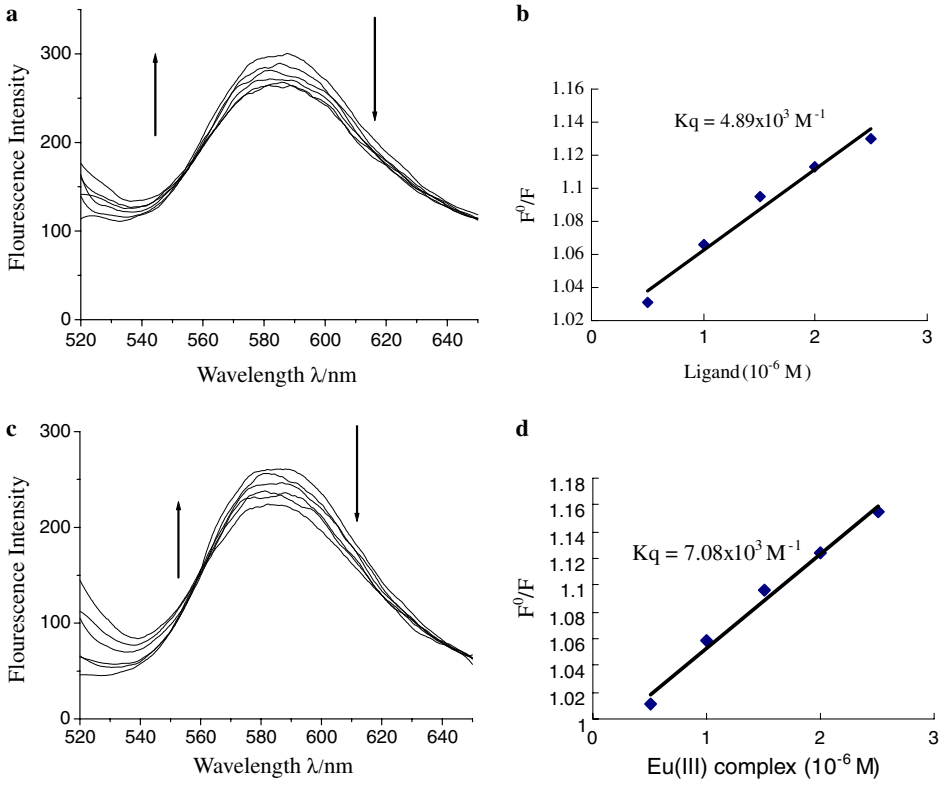

Figure 4. (a) The emission spectra of DNA–EB system (10 and 0.32 μM EB), λ_{ex} = 500 nm, λ_{em} = 520.0–650.0 nm, in the presence of 0, 5, 10, 15, 20, and 25 μM ligand. Arrow shows the emission intensity changes upon increasing ligand concentration. (b) Stern–Volmer plot of the fluorescence titration data of ligand, $K_q = 4.89. \times 10^3\ M^{-1}$. (c) The emission spectra of DNA-EB system (10 and 0.32 μM EB), λ_{ex} = 500 nm, λ_{em} = 520.0–650.0 nm, in the presence of 0, 5, 10, 15, 20, 25 μM Eu(III) complex. Arrow shows the emission intensity changes upon increasing Eu(III) complex concentration. (d) Stern–Volmer plot of the fluorescence titration data of Eu(III) complex, $K_q = 7.08. \times 10^3\ M^{-1}$.

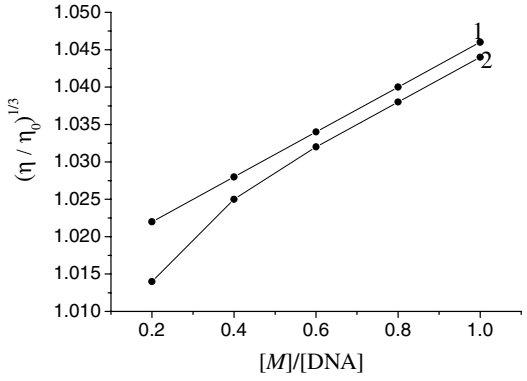

Figure 5. Effect of increasing amounts of Eu(III) complex (line 1) and ligand (line 2) on the relative viscosity of calf-thymus DNA at 25.0 °C.

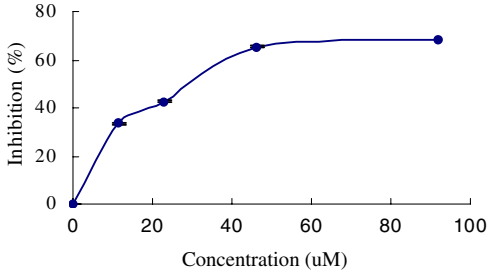

Figure 6. Suppression ratio for $O_2^{-\cdot}$ of **2**.

above absorption titration results. Since these changes indicate only one kind of quenching process, it may be concluded that the Eu(III) complex and free ligand bind DNA via the same mode (intercalation mode).

Table 2. The influence of investigated compounds for $O_2^{-\cdot}$

Compound	Average inhibition (%) for $O_2^{-\cdot}$				IC_{50}^{*} (μM)
	11.5 μM	23 μM	46 μM	92 μM	
L	12.46 ± 0.25	31.23 ± 0.21	46.55 ± 0.23	53.54 ± 0.24	65.06 ± 0.62
1	33.63 ± 0.25	42.67 ± 0.35	65.3 ± 0.36	68.57 ± 0.35	28.46 ± 0.55
2	32.66 ± 0.35	42.46 ± 0.40	52.53 ± 0.42	56.4 ± 0.43	45.53 ± 0.65
3	33.56 ± 0.41	44.6 ± 0.26	61.46 ± 0.25	70.58 ± 0.38	28.08 ± 0.35
4	25.66 ± 0.34	33.63 ± 0.32	47.60 ± 0.40	56.35 ± 0.30	58.89 ± 0.99

Table 3. The influence of investigated compounds for OH·

Compound	Average inhibition (%) for OH·				IC_{50}^{*} (μM)
	11.5 μM	23 μM	46 μM	92 μM	
L	47.60 ± 0.40	63.42 ± 0.38	72.47 ± 0.37	85.54 ± 0.43	12.18 ± 0.24
1	56.40 ± 0.37	68.71 ± 0.36	90.38 ± 0.35	98.44 ± 0.44	8.54 ± 0.15
2	54.64 ± 0.46	75.47 ± 0.37	87.60 ± 0.36	95.62 ± 0.44	7.59 ± 0.22
3	52.32 ± 0.42	69.69 ± 0.52	86.44 ± 0.40	94.43 ± 0.50	9.34 ± 0.04
4	55.47 ± 0.38	72.50 ± 0.48	82.34 ± 0.45	90.64 ± 0.46	7.13 ± 0.04
Mannitol	52.80 ± 0.38	72.45 ± 0.36	90.69 ± 0.38	98.38 ± 0.32	9.17 ± 0.36

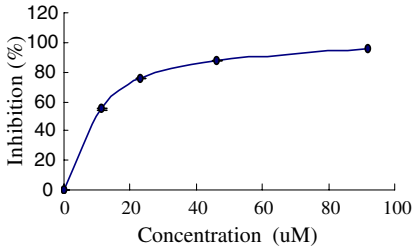

Figure 7. Suppression ratio for OH· of **2**.

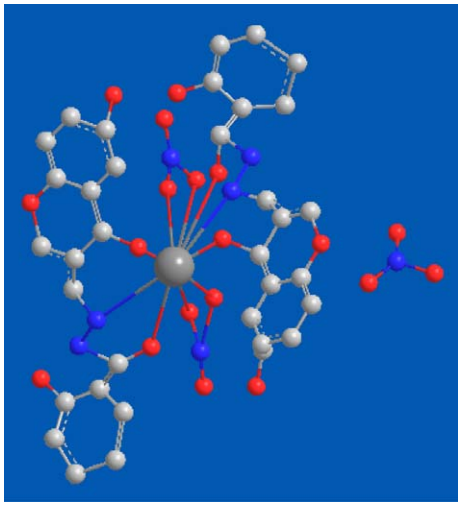

Figure 8. The suggested structure of the complexes.

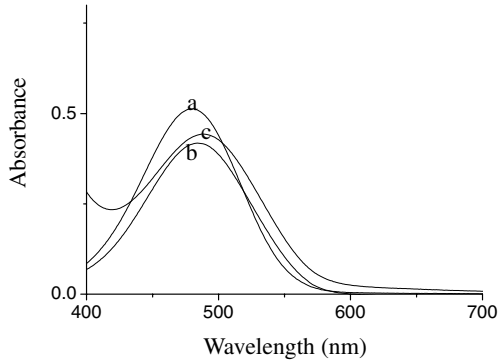

Figure 9. The visible absorption spectra of 1×10^{-5} M EB (a); (a)+1.25×10^{-5} M DNA (b); (b)+2.50×10^{-5} Eu(III) complex (c) in Tris–HCl buffer (5 mM Tris–HCl, 50 mM NaCl, pH 7.1) solution.

Optical photophysical probes generally provide necessary, but not sufficient, clues to support one binding mode. Hydrodynamic measurements that are sensitive to the length change (i.e., viscosity and sedimentation) are regarded as the least ambiguous and most critical tests for binding in solution in the absence of crystallographic structural data.[29] A classical intercalation model demands that the DNA helix lengthens as base pairs are separated to accommodate the binding ligand, leading to an increase in DNA viscosity. In contrast, a partial, non-classical intercalation of compound could bend (or kink) the DNA helix, reducing its effective length and, concomitantly, its viscosity.[30,31] Viscosity experimental results clearly show that both the compounds can intercalate between adjacent DNA base pairs, causing an extension in the helix, and thus increase the viscosity of DNA; and that the Eu(III) complex can intercalate more strongly and deeply than the free ligand, leading to the greater increase in viscosity of the DNA with an increasing concentration of complex. The results obtained from viscosity studies validate those obtained from the spectroscopic studies.

On the basis of all the spectroscopic studies together with the viscosity measurements, we find that the Eu(III) complex and ligand can bind to CT-DNA in an intercalative mode (Fig. 10) and that the Eu(III) complex binds to CT-DNA more strongly than the free ligand.

3.3. Antioxidant activity

It is clear that the scavenger effect on O_2^{-}· can be enhanced by the formation of metal–ligand coordina-

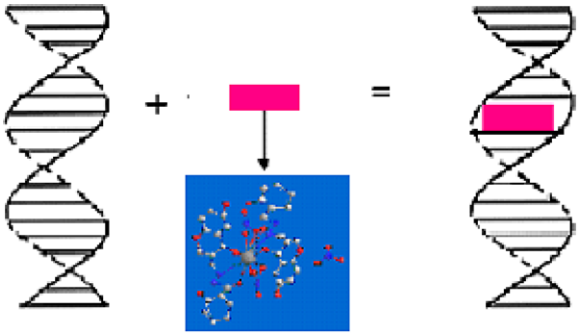

Figure 10. Molecular mode for DNA–Eu-ligand complex (in an intercalative mode).

tion complexes and the nature of the rare earth ions also affects the ability. Some complexes we have synthesized are better effective inhibitor for $O_2^{-\cdot}$ than that of the nitroxide Tempo ($IC_{50} = 60 \pm 3.1$ μM) which has been recently used in biological system for its capacity to mimic superoxide dismutase.[32] Although superoxide is a relatively weak oxidant, it decomposes to form stronger relative oxidative species, such as single oxygen and hydroxyl radicals, which initiate peroxidation of lipids.[33] In the present study, the complexes effectively scavenged superoxide in a concentration-dependent manner. Further, superoxides are also known to indirectly initiate lipid peroxidation as a result of H_2O_2 formation, creating precursors of hydroxyl radicals.[34] These results showed the complexes have significant scavenging activity of superoxide radical and clearly suggested that the antioxidant activity of the complexes was also related to its ability to scavenge superoxide radical.

It is clearly shown that metal complexes exhibit considerable scavenging activity due to the chelation of organic molecule to rare earth ions and rare earth ions such as La(III), Sm(III), Eu(III), and Dy(III) exert differential and selective effects on scavenging radicals of the biological system. Moreover, we find that La (**1**), Sm (**2**), Eu (**3**) complexes are better effective inhibitor for $OH^{\cdot}$ than that of mannitol which is usually used as special scavenger for $OH^{\cdot}$. Therefore, the metal complexes of the free ligand we studied in this paper deserve to be further researched.

4. Conclusion

A new ligand (CDC), 6-hydroxy chromone-3-carbaldehyde-(2′-hydroxy) benzoyl hydrazone, and its four Ln(III) complexes have been prepared and characterized. The DNA-binding properties of the Eu(III) complex and ligand were investigated by absorption, fluorescence, and viscosity measurements. The results support the fact that the compounds bind to CT-DNA via intercalation. The binding constant shows that DNA-binding affinity increases in the order: ligand < Eu(III) complex. All the compounds have shown considerable antioxidant activity, and the suppression rate of the complexes tested is higher than that of the ligand itself. Information obtained from the present work is helpful to the development of nucleic acids molecular probes and new therapeutic reagents for some diseases.

5. Experimental

5.1. Materials

Acetic anhydride, hydroquinone, safranin, and EDTA were produced in China. NBT, MET, $VitB_2$, CT-DNA and EB were purchased from Sigma Chemical Co. All chemicals used were of analytical grade. The rare earth (III) nitrates were derived from their oxide (99.9%) acquired from Nong Hua (PR China). 2-Hydroxy benzoyl hydrazine was prepared according to the literature methods.[35] EDTA–Fe(II) and KH_2PO_4– K_2HPO_4 buffers were prepared with deionized water. All the experiments involving interaction of the Eu(III) complex and the ligand with CT-DNA were carried out in doubly distilled water buffer containing 5 mM Tris and 50 mM NaCl, and adjusted to pH 7.1 with hydrochloric acid. A solution of CT-DNA in the buffer gave a ratio of UV absorbance of about 1.8–1.9:1 at 260 and 280 nm, indicating that the DNA was sufficiently free of protein.[36] The DNA concentration per nucleotide was determined by absorption spectroscopy using the molar absorption coefficient ($6600\ M^{-1}\ cm^{-1}$) at 260 nm.[37] The compounds were dissolved in a mixed solvent of 10% DMF and 90% Tris–HCl buffer (5 mM Tris–HCl, 50 mM NaCl, pH 7.1) at fixed concentration.

5.2. Instrumentation

Carbon, hydrogen, and nitrogen were analyzed on an Elemental Vario EL analyzer. The metal contents of the complex were determined by titration with EDTA. Infrared spectra (4000–400 cm^{-1}) were determined with KBr disks on a Therrno Mattson FTIR spectrometer. The UV–vis spectra were recorded on a Varian Cary 100 Conc spectrophotometer. ^1H NMR spectra were measured on a Varian VR 300-MHz spectrometer, using TMS as a reference in DMSO-d_6. Mass spectra were performed on a VG ZAB-HS (FAB) instrument. The fluorescence spectra were recorded on a Hitachi RF-4500 spectrofluorophotometer. The antioxidative activities of the compounds were tested on a 72 spectrophotometer.

5.3. Preparation of ligand (L)

CDC was prepared according to the literature methods.[17] An ethanol solution containing 2-hydroxy benzoyl hydrazine (1.52 g, 10 mmol) was added dropwise to another ethanol solution containing CDC (1.90 g, 10 mmol). The mixture was stirred for 2 h at room temperature and a white precipitate formed. The precipitate was collected by filtration and washed with ethanol. Recrystallisation from 1:1 (v/v) DMF/H_2O gave the ligand (L), which was dried in a vacuum. Yield: 90%. Mp 256 −258 °C. FAB-MS: $m/z = 325\ [M+H]^+$. Anal. Calcd for $C_{17}H_{12}N_2O_5$: C, 62.96; H, 3.7; N, 21.47. Found: C, 62.12; H, 3.78; N, 21.02. ^1H NMR (DMSO-d_6 300 MHz): δ 11.68 (1H, br, NH), 10.14 (1H, s, a-OH), 10.09 (1H, s, b-OH), 8.72 (1H, s, 2-H), 8.56 (1H, s, CH=N), 7.81–6.82 (7H, m, PhH, 5, 7, 8-H). IR ν_{max} (cm^{-1}): $\nu_{(carbonyl)C=O}$: 1624, $\nu_{(hydrazonic)C=O}$: 1646, $\nu_{C=N}$: 1596 cm^{-1}. U_{max}: (nm) 244, 294, 321.

5.4. Preparation of complexes

The ligand (1.0 mmol, 0.324 g) and the La(III) nitrate (0.5 mmol, 0.217 g) were added together in ethanol (10 mL). The mixtures were stirred at 60 °C. After 5 min, the mixtures, solution was filtered to remove residue and continued stirring for 24 h at room temperature. A white precipitate, the La(III) complex, was separated from the solution by suction filtration, purified by washing several times with ethanol, and dried for 24 h in a vacuum. Sm(**2**), Dy(**3**), and Eu(**4**) complex-

es were prepared by the same way. Anal. Calcd for complex **1** $C_{34}H_{24}N_7O_{19}La$: C, 41.45 (41.94); H, 2.23 (2.46); N, 10.02 (10.07); La, 14.35 (14.27). Λ_m ($S\,cm^2\,mol^{-1}$): 102. IR ν_{max} (cm^{-1}): $\nu_{(carbonyl)C=O}$: 1609, $\nu_{(hydrazonic)C=O}$: 1634, $\nu_{C=N}$: 1566, ν_{NO_3}: 1479, 1383, 1324, 1187, 840. U_{max} (nm): 245, 294, 325. Thermal analyses: T_{decomp} (°C): 237, 315, 392; Residue calcd (%): 15.99 (16.74). Anal. Calcd for complex **2** $C_{34}H_{24}N_7O_{19}Sm$: C, 41.56 (41.45); H, 2.35 (2.44); N, 10.08 (9.96); Sm, 15.52 (15.27). Λ_m ($S\,cm^2\,mol^{-1}$): 112. IR ν_{max} (cm^{-1}): $\nu_{(carbonyl)C=O}$: 1609, $\nu_{(hydrazonic)C=O}$: 1635, $\nu_{C=N}$: 1570, ν_{NO_3}: 1479, 1383, 1324, 1187, 838. U_{max} (nm): 244, 294, 325. Thermal analyses: T_{decomp} (°C): 238, 316, 391; Residue Calcd (%): 17.19 (17.71). Anal. Calcd for complex **3** $C_{34}H_{24}N_7O_{19}Dy$: C, 40.20 (40.94); H, 2.32 (2.41); N, 10.09 (9.83); Dy, 16.85 (16.31). Λ_m ($S\,cm^2\,mol^{-1}$): 102. IR ν_{max}(cm^{-1}): $\nu_{(carbonyl)C=O}$: 1609, $\nu_{(hydrazonic)C=O}$: 1634, $\nu_{C=N}$: 1571, ν_{NO3}: 1479, 1383, 1323, 1187, 840. U_{max} (nm): 245, 293, 324. Thermal analyses: T_{decomp} (°C): 237, 315, 392; Residue Calcd (%): 18.24 (18.71). Anal. Calcd for complex **4** $C_{34}H_{24}N_7O_{19}Eu$: C, 41.67 (41.38); H, 2.35 (2.43); N, 9.79 (9.94); Eu, 16.14 (15.41). Λ_m ($S\,cm^2\,mol^{-1}$): 104. IR ν_{max} (cm^{-1}): $\nu_{(carbonyl)C=O}$: 1609, $\nu_{(hydrazonic)C=O}$: 1635, $\nu_{C=N}$: 1572, ν_{NO_3}: 1479, 1383, 1324, 1186, 838. U_{max} (nm): 245, 294, 325. Thermal analyses: T_{decomp} (°C): 237, 316, 390; Residue Calcd (%): 17.15 (17.84).

5.5. An absorption titration

Absorption titration experiment was performed with fixed concentrations of the drugs, while gradually increasing concentration of DNA. While measuring the absorption spectra, an equal amount of DNA was added to both compound solution and the reference solution to eliminate the absorbance of DNA itself. From the absorption titration data, the binding constant was determined using[38]

$$[DNA]/(\varepsilon_A - \varepsilon_F) = [DNA]/(\varepsilon_0 - \varepsilon_F) + 1/K_b(\varepsilon_0 - \varepsilon_F),$$

where [DNA] is the concentration of DNA in base pairs, ε_A corresponds to the extinction coefficient observed (A_{obsd}/[M]), ε_F corresponds to the extinction coefficient of the free compound, ε_0 is the extinction coefficient of the compound when fully bound to DNA, and K_b is the intrinsic binding constant. The ratio of slope to intercept in the plot of [DNA]/($\varepsilon_A - \varepsilon_F$) versus [DNA] gives the values of K_b.

5.6. Fluorescence spectra

To compare quantitatively the affinity of the compound bound to DNA, the intrinsic binding constants K_b of the two compounds to DNA were obtained by the luminescence titration method. Fixed amounts of compound were titrated with increasing amounts of DNA, over a range of DNA concentrations from 2.5 to 20.0 μM. An excitation wavelength of 326 nm was used, and total fluorescence emission intensity was monitored at 449 nm for Eu(III) complex and 410 nm for ligand. The concentration of the bound compound was calculated using Eq. 1:[23]

$$C_b = C_t[(F - F^0)/(F^{max} - F^0)] \quad (1)$$

where C_t is the total compound concentration, F is the observed fluorescence emission intensity at given DNA concentration, F^0 is the intensity in the absence of DNA, and F^{max} is the fluorescence of the totally bound compound. Binding data were cast into the form of a Scatchard plot[39] of r/C_f versus r, where r is the binding ratio $C_b/[DNA]_t$ and C_f is the free ligand concentration. All experiments were conducted at 20 °C in a buffer containing 5 mM Tris–HCl (pH 7.1) and 50 mM NaCl concentrations.

Further support for Eu(III) complex and ligand binding to DNA by intercalation mode is given through the emission quenching experiment. EB is a common fluorescent probe for DNA structure and has been employed in examinations of the mode and process of metal complex binding to DNA.[40] A 2 mL solution of 10 μM DNA and 0.33 μM EB (at saturating binding levels[41]) was titrated by 5–30 μM Eu(III) complex and ligand (λ_{ex} = 500 nm, λ_{em} = 520.0–650.0 nm).

According to the classical Stern–Volmer equation:[42]

$$F_0/F = K_q[Q] + 1$$

Where F_0 is the emission intensity in the absence of quencher, F is the emission intensity in the presence of quencher, K_q is the quenching constant, and [Q] is the quencher concentration. The shape of Stern–Volmer plots can be used to characterize the quenching as being predominantly dynamic or static. Plots of F_0/F versus [Q] appear to be linear and K_q depends on temperature.

5.7. Viscosity measurements

Viscosity experiments were conducted on an Ubbdlodhe viscometer, immersed in a thermostated water-bath maintained to 25.0 °C. Titrations were performed for the Eu(III) complex and the ligand (1–5 μM), and each compound was introduced into DNA solution (5 μM) present in the viscometer. Data were presented as $(\acute{\eta}/\acute{\eta}_0)^{1/3}$ versus the ratio of the concentration of the compound and DNA, where $\acute{\eta}$ is the viscosity of DNA in the presence of compound and $\acute{\eta}_0$ is the viscosity of DNA alone. Viscosity values were calculated from the observed flow time of DNA containing solution corrected from the flow time of buffer alone (t_0), $\acute{\eta} = t - t_0$.[43,29]

5.8. Scavenger measurements of $O_2^{-\cdot}$

The superoxide radicals ($O_2^{-\cdot}$) were produced by the system of MET/VitB$_2$/NBT.[44] The amount of $O_2^{-\cdot}$ and suppression ratio for $O_2^{-\cdot}$ can be calculated by measuring the absorbance at 560 nm. The solution of MET, VitB$_2$, and NBT was prepared with 0.067 M phosphate buffer (pH 7.8) at avoiding light. The tested compounds were dissolved in DMF. The 10 mL reaction mixture contained MET (0.01 mol/L), NBT (4.6×10^{-5} mol/L), VitB$_2$ (3.3×10^{-6} mol/L), and the tested compound. After illuminating with a fluorescent lamp at 30 °C for 10 min, the absorbance (A_i) of the samples was measured at 560 nm. The sample without the tested compound was used as the control and its absorbance was

A_0. The suppression ratio for $O_2^{-\cdot}$ was calculated from the following expression:

$$\text{Suppression ratio} = 100\frac{A_0 - A_i}{A_0} \quad (2)$$

where A_i = the absorbance in the presence of the ligand or its complexes, A_0 = the absorbance in the absence of the ligand or its complexes.

5.9. Hydroxyl radical scavenging activity

The hydroxyl radical in aqueous media was generated through the Fenton reaction.[45] The solution of the tested compound was prepared with DMF. The sample contained 1 mL of 0.15 M phosphate buffer (pH 7.4), 1 mL of 40 μg/mL safranin, 1 mL of 0.945 mmol/L EDTA–Fe(II), 1 mL of 3% H_2O_2, and 0.5 mL of the solution of the tested compound. The tested samples were kept to react for 0.5 h at constant 37 °C. The absorbances (A_i, A_0) of the samples and a control were measured at 520 nm. The suppression ratio for $OH^{\cdot}$ was calculated from the following expression:

$$\text{Suppression ratio} = 100\frac{A_i}{A_0} \quad (3)$$

where A_i = the absorbance in the presence of the ligand or its complexes, A_0 = the absorbance in the absence of the compound tested and EDTA–Fe(II).

Acknowledgments

This work was supported by the National Natural Science Foundation of China (20475023) and Gansu NST (3ZS 041-A25-016).

References and notes

1. Barton, D.; Ollis, W. D.. In *Comprehensive Organic Chemistry*; Pergamon: Oxford, 1979; Vol 4.
2. Ya Sosnovskikh, V. *Russ. Chem. Rev.* **2003**, *72*, 489; Ellis, G. P.. In *The Chemistry of Heterocyclic Compounds*; Wiley: New York, 1977; Vol. 31, p 749.
3. Horton, D. A.; Bourne, G. T.; Smythe, M. L. *Chem. Rev.* **2003**, *103*, 893.
4. Hadjeri, M.; Barbier, M.; Ronot, X.; Mariotte, A. M. A.; Boumendjel, J.; Boutonnat, J. *Med. Chem.* **2003**, *46*, 2125.
5. Ellis, G. P.; Barker, G. *Prog. Med. Chem.* **1972**, *9*, 65.
6. Erkkila, K. E.; Odom, D. T.; Barton, J. K. *Chem. Rev.* **1999**, *99*, 2777–2796.
7. Lippard, S. J. *Acc. Chem. Res.* **1979**, *11*, 211.
8. Kumar, C. V.; Barton, J. K.; Turro, N. J. *J. Am. Chem. Soc.* **1985**, *107*, 5518–5523.
9. Xu, H.; Zheng, K. C.; Deng, H.; Lin, L. J.; Zhang, Q. L.; Ji, L. N. *Dalton. Trans.* **2003**, *3*, 2260–2268.
10. Mahadevan, S.; Palaniandavar, M. *Inorg. Chim. Acta* **1997**, *254*, 291–302.
11. Xu, H.; Zheng, K. C.; Deng, H.; Lin, L. J.; Zhang, Q. L.; Ji, L. N. *New J. Chem.* **2003**, *27*, 1255–1263.
12. Mozaar, A.; Elham, S.; Bijan, R.; Leila, H. *New J. Chem.* **2004**, *28*, 1227–1234.
13. Chaires, J. B. *Biopolymers* **1998**, *44*, 201–215.
14. Wang, B. D.; Yang, Z. Y.; Wang, Y. *Synth. React. Inorg. Met.-Org. Nano-Met. Chem.* **2005**, *35*, 533–539.
15. Wang, B. D.; Yang, Z. Y.; Wang, Q.; Cai, T. K.; Crewdson, P. *Bioorg. Med. Chem.* **2006**, *14*, 1880–1888.
16. Geary, W. J. *Coord. Chem. Rev.* **1971**, *7*, 1–122.
17. Wang, B. D.; Yang, Z. Y.; Zhang, D. W.; Wang, Y. *Spectrochim. Acta Part A* **2006**, *63*, 213–219.
18. Lehn, J. M. *Angew. Chem., Int. Ed. Engl.* **1990**, *29*, 1304.
19. Latva, M.; Takalo, H.; Simberg, K.; Kankare, J. *J. Chem. Soc., Perkin Trans. 2* **1995**, 995.
20. Kelly, J. M.; Murphy, M. J.; McConnell, D. J.; OhUigin, C. *Nucleic Acids Res.* **1985**, *13*, 167–184.
21. Bloomfield, V. A.; Crothers, D. M.; Tinico, I., Jr. In *Physical Chemistry of Nucleic Acids*; Harper and Row: New York, 1974; p 187.
22. Wilson, W. D.; Ratmeyer, L.; Zhao, M.; Stekowski, L.; Boykin, D. *Biochemistry* **1993**, *32*, 4098–4104.
23. Satyanarayana, S.; Dabrowiak, J. C.; Chaires, J. B. *Biochemistry* **1992**, *31*, 9319–9324.
24. LePecp, J. B.; Paoletti, C. *J. Mol. Biol.* **1967**, *27*, 87–106.
25. Baguley, B. C.; Lebret, M. *Biochemistry* **1984**, *23*, 937–943.
26. Lakowicz, J. R.; Webber, G. *Biochemistry* **1973**, *12*, 4161–4170.
27. Zeng, Y. B.; Yang, N.; Liu, W. S.; Tang, N. *J. Inorg. Biochem.* **2003**, *97*, 258–264.
28. Kumar, C. V.; Barton, J. K.; Turro, N. J. *J. Am. Chem. Soc.* **1985**, *107*, 5518.
29. Michael, T. C.; Marisol, R.; Allen, J. B. *J. Am. Chem. Soc.* **1989**, *111*, 8901–8911.
30. Xiong, Y.; He, X. F.; Zou, X. H.; Wu, J. Z.; Chen, X. M.; Ji, L. N.; Li, R. H.; Zhou, J. Y.; Yu, R. B. *J. Chem. Soc., Dalton Trans.* **1999**, *1*, 19–23.
31. Satyanarayana, S.; Dabrowiak, J. C.; Chaires, J. B. *Biochemistry* **1993**, *32*, 2573–2584.
32. Samuni, A.; Krisna, M. C. In *Handbook of Synthetic Antioxidants*; Packer, L., Cadenas, E., Eds.; Marcel Dekker: New York, 1997; pp 351–373.
33. Dahl, M. K.; Richardson, T. *J. Dairy Sci.* **1978**, *61*, 400.
34. Meyer, A. S.; Isaksen, A. *Trends Food Sci. Technol.* **1996**, *6*, 300.
35. Yu, J. X.; Liu, F. M.; Lu, W. J. *Chin. J. Org. Chem.* **2002**, *20*, 74.
36. Marmur, J. *J. Mol. Biol.* **1961**, *3*, 208.
37. Kumar, C. V.; Asuncion, E. H. *J. Am. Chem. Soc.* **1993**, *115*, 8547–88553.
38. Pyle, A. M.; Rehmann, J. P.; Meshoyrer, R.; Kumar, C. V.; Turro, N. J.; Barton, J. K. *J. Am. Chem. Soc.* **1989**, *111*, 3053–3063.
39. Howe, G. M.; Wu, K. C.; Bauer, W. R. *Biochemistry* **1976**, *19*, 339–347.
40. Kumar, C. V.; Barton, J. K.; Turro, M. J. *J. Am. Chem. Soc.* **1985**, *107*, 5518–5523.
41. Barton, J. K.; Danishefsky, A. T.; Golderg, J. M. *J. Am. Chem. Soc.* **1984**, *106*, 2172–2176.
42. Efink, M. R.; Ghiron, C. A. *Anal. Biochem.* **1981**, *114*, 199–206.
43. Eriksson, M.; Leijon, M.; Hiort, C.; Norden, B.; Gradsland, A. *Biochemistry* **1994**, *33*, 5031–5040.
44. Winterbourn, C. C. *Biochem. J.* **1979**, *182*, 625–628.
45. Winterbourn, C. C. *Biochem. J.* **1981**, *198*, 125–131.